

# FUSE AND HST STIS OBSERVATIONS OF HOT AND COLD GAS IN THE AB AURIGAE SYSTEM

A. ROBERGE<sup>1</sup>, A. LECAVELIER DES ETANGS<sup>2</sup>, C. A. GRADY<sup>3</sup>, A. VIDAL-MADJAR<sup>2</sup>, J.-C. BOURET<sup>3</sup>,  
 P. D. FELDMAN<sup>1</sup>, M. DELEUIL<sup>4</sup>, M. ANDRE<sup>1</sup>, A. BOGGESE<sup>5</sup>, F. C. BRUHWEILER<sup>5</sup>, R. FERLET<sup>2</sup>,  
 AND B. WOODGATE<sup>3</sup>

akir@pha.jhu.edu, lecaveli@iap.fr, cgrady@echelle.gsfc.nasa.gov, mandre@pha.jhu.edu, magali.deleuil@astrsp-mrs.fr, pdf@pha.jhu.edu,  
 ferlet@iap.fr, alfred@iap.fr, woodgate@stis.gsfc.nasa.gov

Draft version October 29, 2018

## ABSTRACT

We present the first observations of a Herbig Ae star with a circumstellar disk by the *Far Ultraviolet Spectroscopic Explorer* (*FUSE*), as well as a simultaneous observation of the star obtained with the *Hubble Space Telescope* Space Telescope Imaging Spectrograph (STIS). The spectra of AB Aurigae show emission and absorption features arising from gases that have a wide range in temperature, from hot O VI emission to cold H<sub>2</sub> and CO absorption. Emissions from the highly ionized species O VI and C III present in the *FUSE* spectrum are redshifted, while absorption features arising from low-ionization species like O I, N I, and Si II are blueshifted and show characteristic stellar wind line-profiles. We find the total column density of H<sub>2</sub> toward AB Aur from the *FUSE* spectrum,  $N(\text{H}_2) = (6.8 \pm 0.5) \times 10^{19} \text{ cm}^{-2}$ . The gas kinetic temperature of the H<sub>2</sub> derived from the ratio  $N(J=1)/N(J=0)$  is  $65 \pm 4 \text{ K}$ . The column density of the CO observed in the STIS spectrum is  $N(\text{CO}) = (7.1 \pm 0.5) \times 10^{13} \text{ cm}^{-2}$ , giving a CO/H<sub>2</sub> ratio of  $(1.04 \pm 0.11) \times 10^{-6}$ . We also use the STIS spectrum to find the column density of H I, permitting us to calculate the total column density of hydrogen atoms, the fractional abundance of H<sub>2</sub>, and the gas-to-dust ratio.

*Subject headings:* stars: individual (AB Aurigae)—stars: atmospheres—circumstellar matter

## 1. INTRODUCTION

AB Aurigae (HD 31293) is one of the brightest and best studied Herbig Ae stars, which are considered to be pre-main-sequence stars of intermediate mass (about 2 – 10 M<sub>⊙</sub>) (Waters & Waelkens 1998). The star (spectral type A0Ve+sh) is about 2 Myr old and is located at a distance of  $144^{+23}_{-17} \text{ pc}$  from the Sun (van den Ancker et al. 1998). Like most Herbig Ae/Be stars, AB Aur is surrounded by circumstellar gas and dust, some of which is distributed in a disk about the star. Standard stellar theory predicts that Herbig Ae/Be stars should not have convective layers, and therefore, should not have chromospheres, coronae, or strong stellar winds. However, AB Aur and most other Herbig Ae/Be stars do show chromospheric and wind features (Böhm & Catala 1993). The *Far Ultraviolet Spectroscopic Explorer* (*FUSE*) provides high-resolution access to a portion of the AB Aur spectrum previously observed only at low spectral resolution with the *Hopkins Ultraviolet Telescope*. In this Letter, we present *FUSE* observations of AB Aur, including the first observation of hot O VI gas ( $T \approx 3 \times 10^5 \text{ K}$ ) and cold molecular hydrogen. The O VI emission should provide an important constraint on any models of the stellar activity seen in the AB Aur system. We also present a simultaneous observation of AB Aur with the *Hubble Space Telescope* (*HST*) Space Telescope Imaging Spectrograph (STIS); this observation strongly complements the *FUSE* observations by providing column

densities of H I and CO.

## 2. FUSE OBSERVATIONS AND DATA REDUCTION

AB Aurigae was observed with *FUSE* on 2000 February 27 and 28, for a total exposure time of 13.7 ks. The data were obtained using the low-resolution aperture (LWRS), and alignment of the four channels (LiF 1, LiF 2, SiC 1, and SiC 2) was maintained throughout the whole observation (see Sahnou et al. (2000) for a more detailed explanation). The data were flux calibrated using *calfuse 1.6.8* pipeline processing software, but more recent wavelength solutions (2000 June 19) were used for our analysis. We obtained a S/N of about 5 per 12-pixel resolution element in the LiF 1a segment (near 1060 Å), and about 7 in the LiF 1b segment (near 1140 Å).

The wavelength solutions used provide good relative calibration across the LiF channels. However, they have significant zero-point offsets. In order to establish the absolute wavelength calibration of our spectra, we made use of the simultaneous STIS observation of AB Aur described in §5. Assuming that our H<sub>2</sub> gas is located in the same region and is at the same velocity as the carbon monoxide gas observed in the STIS spectrum, we set  $v_{\text{H}_2} = v_{\text{CO}} = 10 \pm 3 \text{ km s}^{-1}$ , which is close to the heliocentric radial velocity of the star ( $v_{\text{rad}} = 8 \text{ km s}^{-1}$ ).

## 3. ANALYSIS OF FUSE SPECTRUM

<sup>1</sup> Department of Physics and Astronomy, Johns Hopkins University, Baltimore, Maryland 21218

<sup>2</sup> Institut d'Astrophysique de Paris, CNRS, 98bis Bd Arago, F-75014 Paris, France

<sup>3</sup> NASA/Goddard Space Flight Center, Code 685, Greenbelt, Maryland 20771

<sup>4</sup> Laboratoire d'Astronomie de Marseille, BP 8, F-13376 Marseille Cedex 12, France

<sup>5</sup> Institute for Astrophysics & Computational Sciences, Department of Physics, The Catholic University of America, Washington, DC 20064

The spectrum in Figure 1a shows signal from AB Aur down to C III at 977 Å, and is rich in emission and absorption features, many of which we have not yet been able to identify. The stellar photosphere flux drops off sharply at around 1270 Å (Figure 1b), so virtually all the observed flux in the *FUSE* bandpass is due to a forest of emission lines and possibly some far-UV excess continuum of uncertain origin.

### 3.1. Emission from highly-ionized species O VI and C III

The O VI emission doublet in the LiF 1a segment spectrum is shown in Figure 2a. The  $\lambda 1038$  line is suppressed by H<sub>2</sub> absorption; two narrow H<sub>2</sub> lines are also superimposed on the  $\lambda 1032$  line. These two narrow lines were masked out of the data, and a Gaussian model was least-squares fitted to the spectrum between 1029 Å and 1035 Å. A model for the O VI doublet was created using this Gaussian fit, assuming the optically thin line ratio 2:1 to model the  $\lambda 1038$  line. This O VI model was multiplied by the normalized H<sub>2</sub> absorption model discussed in §3.2; the result is overplotted on the data in Figure 2a, showing how the strong H<sub>2</sub> absorption lines near 1037 Å and 1039 Å cut off the wings of the  $\lambda 1038$  line, reproducing the peculiar line shape quite well. However, this analysis indicates that there should be additional flux visible at 1038.8 Å; absorption from some other atomic species may be responsible for the lack of observed emission. The Gaussian fit to the  $\lambda 1032$  line is redshifted ( $v = 105 \pm 11$  km s<sup>-1</sup>, corrected for the zero-point offset of the wavelength calibration), with a FWHM =  $356 \pm 11$  km s<sup>-1</sup>.

The O VI line profile does not appear to be a standard type I P Cygni profile (Beals 1950), because no blueshifted absorption is observed on the small but significant continuum flux around the emission line. While the Gaussian model fits the red wing of the  $\lambda 1032$  line quite well, there is excess emission on the blue wing. This asymmetry in the line-profile suggests that the O VI emission is formed in AB Aur’s stellar wind, but this conclusion is tentative until more detailed modeling is complete.

The C III  $\lambda 977$  line in the SiC 1b segment spectrum is shown in Figure 2b. Again, there are narrow H<sub>2</sub> absorption lines superimposed on the emission feature, which were masked out before least-squares fitting a Gaussian to the line. The bulk of the emission is redshifted ( $v = 192 \pm 11$  km s<sup>-1</sup>), but the C III emission feature clearly is not well-described by a single Gaussian. There is an “absorption feature” at  $\sim 978$  Å, superimposed on the C III emission, that does not arise from H<sub>2</sub>. The origin of this feature has not yet been determined, but it is not likely to be interstellar, because of its large redshift and width.

### 3.2. Molecular hydrogen

The H<sub>2</sub> absorption features visible in our *FUSE* spectrum do not show any evidence of multiple velocity components. The LiF 1a and LiF 2a data were normalized with simple continua found from linear fits to the spectrum between 1040 Å and 1120 Å. Our H<sub>2</sub> absorption model was generated using molecular data from Abgrall et al. (1993a) and Abgrall et al. (1993b). Voigt line-profiles were used to create transmission functions, which were then convolved with a Gaussian instrumental line-spread function with  $FWHM = \lambda/15000$ . The  $\chi^2$  statistic between the model

and the data was minimized to find the best model parameters, with 1- $\sigma$  error bars determined from the contours of  $\chi^2$ . The velocity of the gas was found by least-squares fitting Gaussians to a number of narrow lines between 1050 Å and 1120 Å. We measured  $v_{H_2} = 103 \pm 10$  km s<sup>-1</sup>, but set this value to the STIS carbon monoxide velocity,  $v_{CO} = 10 \pm 3$  km s<sup>-1</sup>, to determine the zero-point offset of our wavelength calibration.

Since the relative populations of H<sub>2</sub> energy levels with  $\nu = 0$  and  $J = 0, 1$  are determined primarily by thermal collisions, the excitation temperature found from these levels should be close to the kinetic temperature of the gas. However, the populations of the higher levels ( $J \geq 2$ ) can be inflated by UV and/or formation pumping and by radiative cascade (Shull & Beckwith 1982). Therefore, the low  $J$  and high  $J$  levels were analyzed separately. Windows containing only lines arising from the  $J = 0, 1, 2$  levels in the five bands between 1048 Å and 1120 Å were cut out of the normalized LiF 1a and LiF 2a data and  $\chi^2$  minimization performed using a model containing only these lines. We permitted the model to have a slightly different velocity shift for each of the windows, to eliminate any systematic errors arising from the uncertainty in the H<sub>2</sub> velocity determination. The parameters of the model were  $N(J = 0)$ ,  $N(J = 1)$ ,  $N(J = 2)$ , the column densities in the  $J = 0, 1, 2$  levels respectively, and  $b$ , the Doppler broadening parameter. From the ratio  $N(J = 1)/N(J = 0)$ , we calculate the gas kinetic temperature of the H<sub>2</sub>,  $T = 65 \pm 4$  K. To analyze the high  $J$  lines, we again cut windows containing only lines arising from  $J \geq 2$  out of the data, and performed  $\chi^2$  minimization using a model containing only those lines. We find the excitation temperature of the high  $J$  lines to be  $212 \pm 20$  K. The column densities of molecules in each rotational level were summed to find the total H<sub>2</sub> column density,  $N(H_2) = (6.8 \pm 0.5) \times 10^{19}$  cm<sup>-2</sup>. The final best two-temperature model is shown overplotted on a portion of the LiF 1a spectrum in Figure 3a.

## 4. STIS OBSERVATION AND DATA REDUCTION

AB Aur was observed by *HST* on 2000 February 28. A total exposure time of 1813 s was obtained using the E140M echelle grating and the  $0.''2 \times 0.''06$  spectroscopic slit. The spectrum covered 1150–1725 Å with a resolution of  $\approx 46,000$ . The data were reduced using the STIS IDT software *calstis*. Echelle spectra are subject to interorder scattered light; to compensate for this, we used the algorithm developed by Don Lindler and discussed in Holberg et al. (1999), which accurately achieves zero flux in the trough of the interstellar Ly $\alpha$  absorption. The STIS wavelength scale in this mode is accurate to 3 km s<sup>-1</sup> (Pagano et al. 2000). The spectrum between 1200 Å and 1300 Å is shown in Figure 1b. Longward of 1300 Å, the spectrum resembles an early A star with the heavy line blanketing typical of Herbig Ae stars in the UV. The STIS spectrum reached a continuum S/N=20.6 near 1471 Å, and S/N=16 near 1504 Å. The S/N at shorter wavelengths is lower, S/N  $\leq 3.8$  per 0.2 Å bin at Lyman  $\alpha$ .

## 5. ANALYSIS OF STIS SPECTRUM

The STIS spectrum of AB Aur is rich in emission lines from a wide range of ionization states. The data short-

ward of 1310 Å show type I P Cygni profiles arising from the low-ionization species O I and N I, and more complex emission profiles in Si III and C III  $\lambda$ 1176.

### 5.1. Extinction, Lyman $\alpha$ , and $N(\text{H I})$

The measured color index of AB Aur,  $(B-V)$ , is 0.12. IUE low-dispersion spectra of AB Aur (SWP 24389) were unreddened using the interstellar extinction law of Cardelli, Clayton, & Mathis (1989). Comparison with unreddened spectral standards suggests that the best overall match in the FUV is  $\gamma$  UMa, type A0 V (SWP 8198), with  $(B-V)_0 = 0.04$  and  $R = 3.1$ . We therefore find the selective extinction toward AB Aur,  $E(B-V) = 0.08$ , and the general extinction,  $A_V = R \times E(B-V) = 0.25$ .

Lyman  $\alpha$  emission is formed in the chromosphere of AB Aur, and it appears likely that the chromosphere is expanding, based on profiles of other low-ionization species. Since these line-profiles in the STIS spectrum of AB Aur are observed to be type I P Cygni profiles, with the emission extending down to the stellar radial velocity, it is likely that the intrinsic Lyman  $\alpha$  profile is a type I P Cygni profile as well. However, the short wavelength edge of the observed emission does not extend down to the stellar radial velocity; this is presumably due to the interstellar Lyman  $\alpha$  absorption. The wavelength at which the interstellar absorption is no longer optically thick, where the observed flux rises above the zero level, is highly sensitive to the interstellar H I column density, but insensitive to the assumed b-value. We find  $N(\text{H I})$  toward the star to be  $3 \times 10^{20} \text{ cm}^{-2}$ . We obtain roughly the same value using several different assumptions about the underlying continuum flux. However, uncertainty about the exact shape of the stellar line-profile could cause the error in this value to be as much as 50%. Future work will refine  $N(\text{H I})$  after detailed modeling of AB Aur's winds determines the unattenuated stellar flux presented to the interstellar H I atoms.

### 5.2. Carbon monoxide

The (1-0), (2-0), and (3-0) bands of the CO Fourth Positive band system ( $A^1\Pi - X^1\Sigma^+$ ) are visible in the STIS spectrum (Figure 3b). No lines arising from  $^{13}\text{CO}$  were observed. The continua in the vicinity of the bands were fitted with fifth-degree polynomials. An absorption model was generated using wavelengths and oscillator strengths from Morton & Noreau (1994) and energies of the ground-state levels were calculated using the Dunham coefficients from Farrenq et al. (1991).  $\chi^2$  minimization was performed on all three bands simultaneously to find the best rotational excitation temperature,  $T_{\text{CO}} = 7.0 \pm 0.7 \text{ K}$ , Doppler broadening parameter,  $b = 3.8 \pm 0.4 \text{ km s}^{-1}$ , column density of  $^{12}\text{CO}$ ,  $N(\text{CO}) = (7.1 \pm 0.5) \times 10^{13} \text{ cm}^{-2}$ , and velocity centroid,  $v = 10 \pm 3 \text{ km s}^{-1}$ .

## 6. DISCUSSION

We find a total column density of hydrogen atoms,  $N_{\text{H}} = N(\text{H I}) + 2N(\text{H}_2) = 4.4 \times 10^{20} \text{ cm}^{-2}$ , which is typical of a diffuse molecular cloud. The fractional abundance

of  $\text{H}_2$ ,  $f = 2N(\text{H}_2)/N_{\text{H}} = 0.31$ . Only 11 out of 91 stars in the Savage et al. (1977) *Copernicus* survey of interstellar  $\text{H}_2$  show a larger value of  $f$ , and these sight-lines all have larger values of  $E(B-V)$  and  $N_{\text{H}}$ . This might suggest that our line-of-sight to AB Aur has an anomalously high molecular fraction, but this conclusion is tentative until further FUSE  $\text{H}_2$  measurements of a variety of interstellar environments are complete. The  $\text{CO}/\text{H}_2$  ratio is  $(1.04 \pm 0.11) \times 10^{-6}$ . We find the gas-to-dust ratio,  $N_{\text{H}}/E(B-V) = 5.5 \times 10^{21}$ . The mean ratio for standard clouds within 2 kpc of the Sun is  $5.9 \times 10^{21}$ , indicating that our gas-to-dust ratio is not atypical (Bohlin et al. 1978).

Optical coronagraphic images of AB Aur show an extended arc of reflection nebulosity to the east of the system, in addition to the circumstellar disk centered on the star (Nakajima & Golimowski 1995; Grady et al. 1999). Nakajima & Golimowski (1995) suggest that such nebulosities are the remnants of the original molecular clouds that collapsed to form low-mass stars. Our values of the various parameters describing the cold  $\text{H}_2$  and CO gases ( $T_{\text{kin}}$ ,  $N_{\text{H}}$ ,  $f$ ,  $\text{CO}/\text{H}_2$  and  $N_{\text{H}}/E(B-V)$ ) are consistent with this suggestion, and we believe that the  $\text{H}_2$  and CO gases toward AB Aur are probably located in a remnant molecular cloud envelope around the star. The fact that the velocity of the CO gas is equal (within measurement error) to the stellar radial velocity supports this conclusion. The molecular gases are not likely to be located in the circumstellar disk around AB Aur, since the disk inclination is such that our line-of-sight to the star does not pass through the disk (Grady et al. 1999).

Turning to the hot, highly-ionized gases, FUV emission lines from O VI and C III are observed in the solar spectrum, and are produced in the transition zone between the chromosphere and the corona. However, detailed modeling of the N V ( $T \approx 1.4 \times 10^5 \text{ K}$ ) emission previously observed from AB Aur with GHRS found that a homogeneous, spherically-symmetric high-temperature zone could not produce the observed N V emission without producing strong N IV or C IV emission as well, which is not seen (Bouret et al. 1997). Bouret et al. (1997) concluded that small, hot clumps, formed by shocks in a stellar wind, could reproduce the FUV emission lines, as well as the weak X-ray flux observed from AB Aur. Future work will determine if the wind-shock model can reproduce the observed emission from C III and the higher-temperature ( $T \approx 3 \times 10^5 \text{ K}$ ) species O VI.

This work is based on observations made with the NASA-CNES-CSA *Far Ultraviolet Spectroscopic Explorer* and on NASA-ESA *Hubble Space Telescope* observations obtained at the STScI under the Guaranteed Time Observer program 8065. FUSE is operated for NASA by the Johns Hopkins University under NASA contract NAS5-32985. The work performed by J.-C. Bouret was supported by a National Research Council-(NASA GSFC) Research Associateship.

## REFERENCES

- Abgrall, H. et al. 1993a, A&AS, 101, 273  
Abgrall, H. et al. 1993b, A&AS, 101, 323  
Beals, C. S. 1950, Publ. DAO, 9, 1  
Bohlin, R. C., Savage, B. D., & Drake, J. F. 1978, ApJ, 224, 132  
Böhm, T. & Catala, C. 1993, A&AS, 101, 629  
Bouret, J.-C., Catala, C., & Simon, T. 1997, A&A, 328, 606  
Cardelli, J. A., Clayton, G. C., & Mathis, J. S. 1989, ApJ345, 245  
Farrenq, R., et al. 1991, J. Mol. Spectrosc., 149, 375  
Grady, C., et al. 1999, ApJ, 523, L151  
Holberg, J., et al. 1999 ApJ, 517, 841  
Morton, D. C. & Noreau, L. 1994, ApJS, 95, 301  
Nakajima, T. & Golimowski, D. A. 1995, AJ, 109, 1181  
Pagano, I., et al. 2000, ApJ, 532, 497  
Sahnow, D. et al. 2000, ApJ, 538, L7  
Savage, B. D., Bohlin, R. C., Drake, J. F., & Budichi, W. 1977, ApJ, 216, 291  
Shull, J. M. & Beckwith, S. 1982, ARA&A, 20, 163  
van den Ancker et al. 1998, A&A, 330, 145  
Waters, L. B. F. M. & Waelkens, C. 1998, A&A Rev., 36, 233

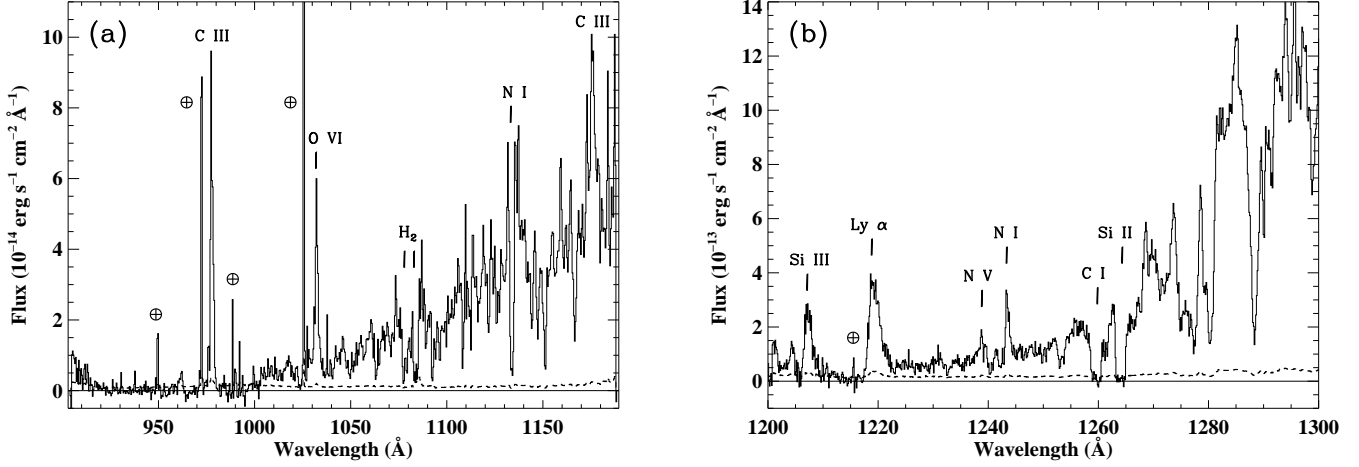


FIG. 1.— Overview of the AB Aurigae FUV spectrum. The  $1 - \sigma$  flux measurement errors are plotted with a dashed line. Airglow lines are indicated by  $\oplus$ , and prominent features are labeled. (a) *FUSE* spectrum of AB Aur, combining data from all channels. The data have been rebinned by a factor of 80 for this plot. (b) Short wavelength portion of the STIS E140M spectrum of AB Aur. The data have been rebinned by a factor of 10 for this plot.

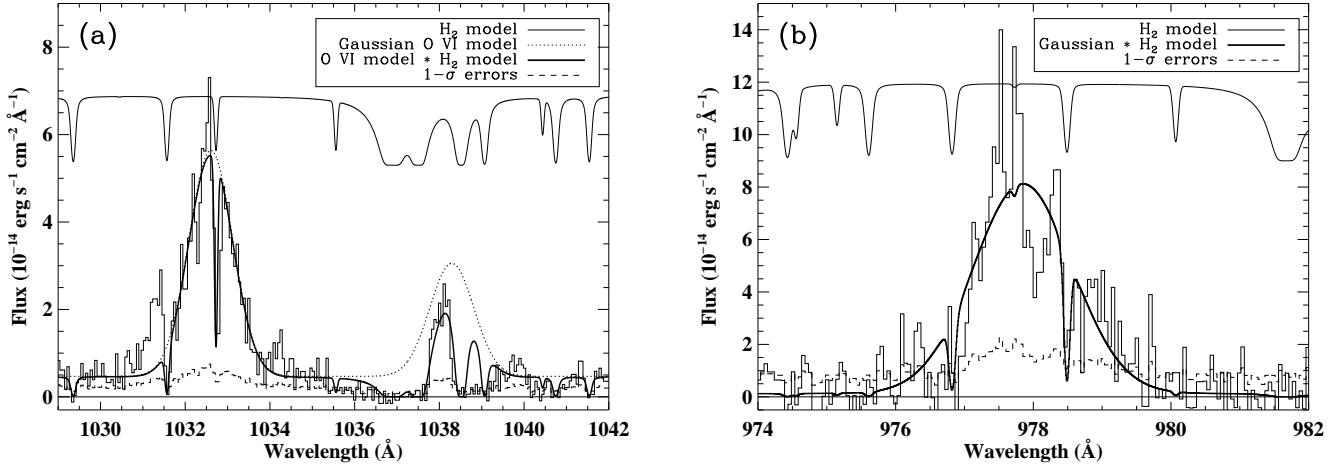


FIG. 2.— Emission from highly-ionized species in the *FUSE* spectrum. The data have been rebinned by a factor of 8 for these plots. Our best  $H_2$  absorption model is shown at the top of both plots. The  $1 - \sigma$  flux measurement errors are plotted with a dashed line. (a) O VI  $\lambda\lambda 1032, 1038$  doublet in the LiF 1a spectrum. An optically thin Gaussian O VI model is shown with a dotted line. The normalized  $H_2$  model was multiplied by the O VI model and overplotted with a thick line. (b) C III  $\lambda 977$  line in the SiC 1b spectrum. Our Gaussian fit to the line multiplied by the  $H_2$  model is overplotted with a thick line.

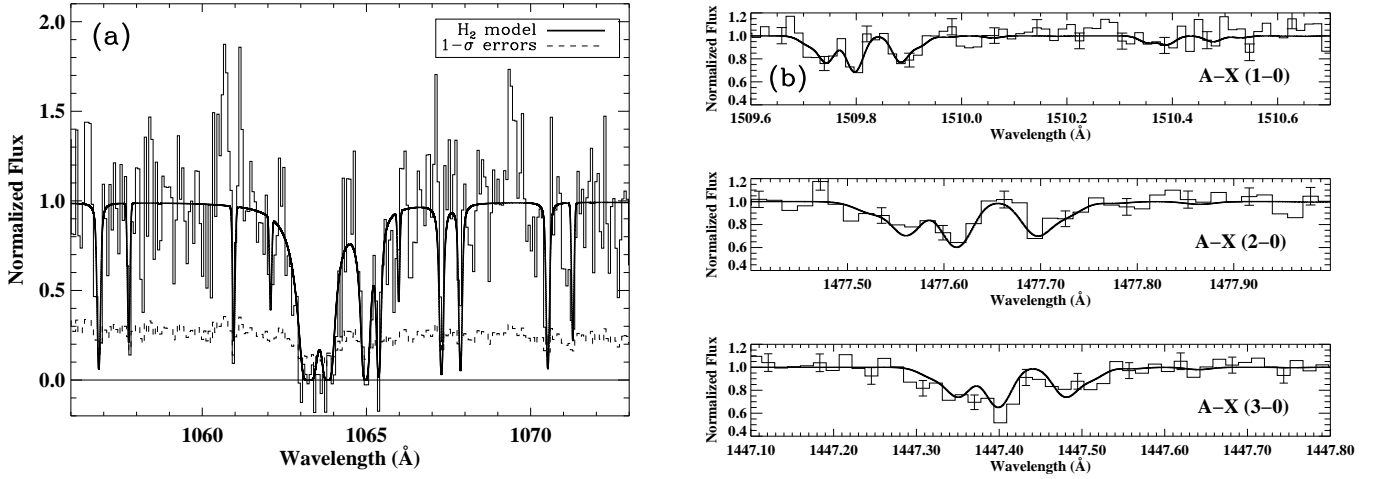


FIG. 3.— Molecular gases toward AB Aur. (a)  $H_2$  Lyman (3-0) band in *FUSE* LiF 1a spectrum. The data have been rebinned by a factor of 10 for this plot. The  $1-\sigma$  flux measurement errors are plotted with a dashed line. The best two-temperature model is overplotted with a thick line. (b) Three bands of the CO Fourth Positive band system in the STIS E140M spectrum. The data have not been rebinned or smoothed for this plot. The  $2-\sigma$  flux error bars are overlaid on the data. The best model is overplotted with a thick line.